Pol. J. Environ. Stud. Vol. 21, No. 5 (2012), 1497-1503

Original Research

Biosorption of Sb(III) to Exopolymers from Cyanobacterium *Synechocystis* sp.: a Fluorescence and FTIR Study

Daoyong Zhang[1], Xiangliang Pan[2]*, Guijin Mu[1]

[1]State Key Laboratory of Environmental Geochemistry, Institute of Geochemistry, Chinese Academy of Sciences, Guiyang, 550002, Guizhou, China
[2]State Key Laboratory of Desert and Oasis Ecology, Xinjiang Institute of Ecology and Geography, Urumqi, 830011, Xinjiang, China

Received: 15 October 2010
Accepted: 14 March 2012

Abstract

Antimony (Sb) pollution in Sb mining areas has been of growing environmental concern. However, limited information is available on environmental behavior and biogeochemical process of Sb. In the present study, complexation of Sb(III) with extracellular polymeric substances (EPS) from cyanobacterium *Synechocystis* sp. was investigated using excitation-emission matrix (EEM) fluorescence spectroscopy. Two protein-like fluorescence peaks were identified in the EEM spectra of EPS. Fluorescence of both peaks was clearly quenched by Sb(III). The quenching constants ($\log K_a$) and the binding constants ($\log K_b$) for peaks A and B were in the range of 3.21-4.13 and 3.22-4.14, respectively. The interaction between EPS and Sb(III) is spontaneous and endothermic. The binding of Sb(III) to EPS is dominated by the hydrogen bonding and Van der waals forces. FTIR analysis showed that polysaccharides in EPS also participated in complexation EPS with Sb(III).

Keywords: binding, extracellular polymeric substances, Sb(III), fluorescence quenching

Introduction

Antimony (Sb) (MW=121.76) is a toxic metal element belonging to subgroup 15 of the periodic table of elements, and has been listed as a prioritary pollutant [1]. Sb is carcinogenic [2] and can cause liver damage, hemolysis, hematuria, apoptosis in human fibroblasts (HFs), sister chromatid exchanges (SCEs), a human bronchial epithelial cell line (BES-6), and circulatory disease [3]. Sb also has been demonstrated to be toxic to microalgae [4] and higher plants [5, 6].

Southwestern China holds more than 80% of the antimony ore reserves of the world and a number of big Sb mines. In this area, Sb pollution is of great environmental concern. Take Xikuangshan (Hunan Province) as an example, where Sb levels in the downstream river water and topsoil around the mine are in the range 5.9-7.6 $mg \cdot L^{-1}$ [7] and up to 5,045 $mg \cdot kg^{-1}$ [8], respectively. The high levels of Sb in the water and soil partly come from the discharged Sb mine drainage, which has not been effectively treated. How to cost-effectively treat the Sb mine drainage is an urgent task for these Sb mines in southwestern China. However, unlike other heavy metals such as Pb, Cd, Zn, and Hg, treatment technologies of Sb mine drainage are limited.

Biosorption is a rapid, efficient, cost-effective, and novel technology for the removal of heavy metals from aqueous solution [9-11]. Various biomaterials, including microorganisms, have been demonstrated to be effective

*e-mail: panxl@ms.xjb.ac.cn

adsorbents for various heavy metal ions [10-14]. Intracellular accumulation, binding to cell walls and complexation with extracellular polymeric substances (EPS) can be involved in biosorption. EPS, excreted by most bacterial species, are mainly made up of polysaccharides, protein, humic substances, and lipids [15]. EPS possess a variety of the groups on its surface such as hydroxy, carboxyl, and amidocyanogen [16]. This makes EPS have strong binding ability to heavy metal ions and some organic pollutants, and thus it plays a major role in biosorption of metal ions [15, 17-22]. Knowledge about biosorption of Sb by microbes and their EPS is lacking.

Our previous study showed that cyanobacterium *Synechocystis* sp. was an effective adsorbent for Sb(III), and their EPS played an important role in biosorption of Sb(III) [22]. In the range of initial Sb concentrations of 5-100 $mg \cdot L^{-1}$, 32.4-48.5% of Sb adsorbed to *Synechocystis* sp. cells were immobilized by EPS. However, more qualitative and quantitative information and mechanisms about biosorption of Sb(III) by the EPS of *Synechocystis* sp. need further study. Therefore, the purpose of the present study was to investigate the biosorption of Sb(III) to EPS from cyanobacterium *Synechocystis* sp. and the stability of EPS-Sb(III) complexes, using EEM (excitation emission matrix) fluorescence spectroscopy and FTIR (Fourier Transform Infrared) spectroscopy.

Materials and Methods

Culture of Cyanobacterium

Synechocystis sp. (FACHB 898) cells were obtained from the Institute of Hydrobiology, Chinese Academy of Sciences. The cells were grown in BG-11 medium [23] at 30ºC under fluorescent white light (55 μmols photons $m^{-2} \cdot s^{-1}$).

Chemicals

Sb(III) solution was prepared by dissolving analytical-grade antimony potassium tartrate in deionized water.

Extraction of EPS

EPS of the cyanobacterial cells was extracted by centrifuge [18, 24], which would not cause cell lysis [18]. The cyanobacterial cells were centrifuged at 4300×g for 10 min at 4ºC in order to remove medium and other solved substances [25]. The residue was re-suspended in high-purity Milli-Q water and EPS were separated by centrifuge at 20,000×g and 4ºC for 20 min. [18]. The supernatants were filtered through 0.22 μm acetate cellulose membranes and stored at 4ºC for use.

Determination of Protein and Polysaccharide Contents

Polysaccharide content in EPS was measured by the phenolsulfuric acid method with glucose as the standard [26]. Protein content in EPS was determined by Bradford method using bovine serum albumin as the standard [27].

EEM Fluorescence Spectroscopy and Fluorescence Titration

The EEM spectra of the EPS solution were recorded with a fluorescence spectrophotometer (F-7000, HITACHI, Japan). The EEM spectra were collected at 5 nm increments over an excitation range of 200-400 nm, with an emission range of 250-550 nm by every 2 nm. The excitation and emission slits were set to 5 and 10 nm of band-pass, respectively. The scan speed was 1,200 $nm \cdot min^{-1}$. The Milli-Q water blank was subtracted from the sample's EEM spectra, and EEM data was processed using the SigmaPlot 2000 (Systat, US) software.

EPS solution with 0.01 M KNO_3 in a 1cm×1cm quartz cuvette was titrated with the incremental additions of 5 μL 0.1 M Sb(III) at 288, 293, and 298 K. In order to examine the effect of solution pH on fluorescence quenching, both the EPS solution and Sb(III) solution were preadjusted to 3, 5, 7, and 9 using 0.1 M HCl and 0.1 M NaOH. After each addition of Sb(III), the solution was mixed using a magnetic stirrer for 15 min. Fluorescence quenching titrations of EPS by Sb(III) at various temperatures were conducted.

FTIR Spectroscopy

The EPS sample was lyophilized. About one milligram of freeze-dried EPS was mixed with 100 mg of KBr and compacted in pellet form. The FTIR spectra of EPS samples were collected by an FTIR spectrometer (Tensor 27, Bruker, German) with 4 cm^{-1} resolution against a KBr background. All spectra were smoothed using the Savitsky-Golay algorithm, and the baseline was corrected using the "automatic baseline correct" function.

Results and Discussion

EEM of EPS in Absence and Presence of Sb(III) at Various pHs

The polysaccharide and protein content in EPS were 2.15 and 6.27 $mg \cdot g^{-1}$ EPS, respectively, with a polysaccharide-to-protein content ratio of about 1:3. Fig. 1a showed the exemplified EEM spectra of EPS from *Synechoeystis* sp. at pH 6. Two fluorescence peaks (peak A with Ex/Em = 265-270/298-308 nm and peak B with Ex/Em = 220-225/ 302-338 nm) were found in the EEM spectrum of EPS, respectively. Peaks A and B could be identified as protein-like substances. Peak A could be further assigned to tyrosine [28-30]. The location of two peaks showed blue-shift in comparison with the previous studies [28, 30, 31]. Fig. 1b showed that fluorescence intensities of peaks A and B were clearly reduced after the addition of 50 μM Sb(III), indicating the interaction of the fluorophores in EPS and Sb(III).

Fig. 2. showed that fluorescence intensities of both peaks decreased under acidic conditions.

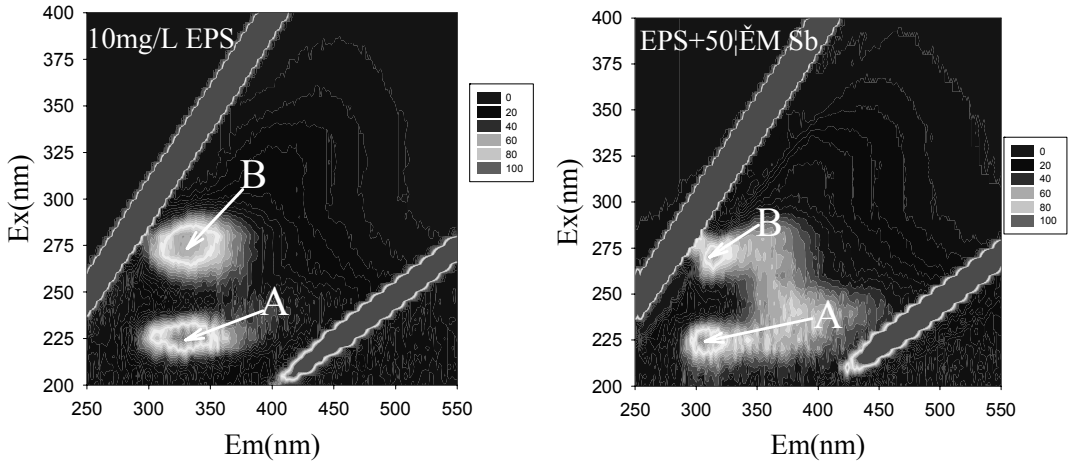

Fig. 1. Exemplified EEM spectra of EPS (a) and EPS + 50 μM Sb(III) (b) at pH 6 and 298 K.

However, under neutral and basic conditions, fluorescence intensities of peak A changed little while fluorescence intensities of peak B were significantly reduced. This shows that fluorophore A (represented by peak A) does not interact with Sb(III) under neutral and basic conditions, whereas fluorophore B interacted with Sb(III) at all experimental pHs. The quenching of fluorescences denoted the binding of Sb(III) to EPS and some fluorescent organic ligands may complex with Sb(III). The maximal fluorescence intensities at peaks A and B before and after the addition of Sb(III) were found at pH 5-7. Fluorescence intensities of both peaks decreased under acidic or basic conditions. This was similar to EPS from natural biofilm and its interaction with Hg(II) [30]. The influence of pH change on fluorescence of EPS might be assigned to the change of the molecular orbit of the excitable electrons and the configuration of protein-like substances (aromatic amino acid residues such as tryptophan, tyrosine, and phenylalanine) [30, 32]. The protein-like fluorophores are unfolded under neutral conditions, whereas some of these fluorophores are masked under acidic and basic conditions, which decreases the fluorescence intensity.

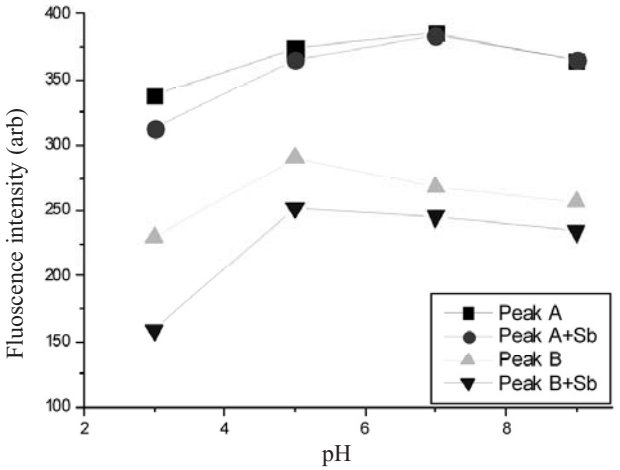

Fig. 2. Fluorescence intensities of both peaks decreased under acidic conditions.

Fluorescence Quenching Mechanism

Generally, the fluorescence quenching process can be divided into static quenching process and dynamic quenching process. The dynamic quenching is attributed to the collision between fluorophore and quencher at excited state while static quenching is assigned to the formation of a complex between fluorophore and quencher with the external forces [33]. In order to understand the mechanisms underlying fluorescence quenching of the various fluorophores in EPS by Sb(III), the fluorescence titration data were analyzed with Stern-Volmer equation (1):

$$F_0/F = 1 + k_q\tau_0[\text{Sb(III)}] = 1 + K_{sv}[\text{Sb(III)}] \quad (1)$$

...where F_0 and F are fluorescence intensities of the fluorophores in the absence and presence of Sb(III), respectively; k_q is energy transfer rate ($M^{-1}\cdot s^{-1}$); τ_0 refers to lifetime of fluorescence (s), taken as 10^{-8} s [33]; K_{sv} is the Stern-Volmer constant; and [Sb(III)] is the concentration of Sb(III).

If there is good relationship for plot of F_0/F versus [Sb(III)], the fluorescence quenching may be governed by either static quenching or dynamic quenching singly [33].

It was found that all the Stern-Volmer plots clearly showed concave-down features for peaks A and B at pHs of 4, 6, and 8 (Fig. 3). The concave-down curve suggests that there are two fluorophore populations at an individual peak [33]. One population is accessible to the quencher and the other is not accessible to the quencher, indicating that only the florescence from the accessible fluorophore has the potential to be quenched.

The modified Stern-Volmer equation was further employed to describe fluorescence quenching titration data. The observed fluorescence intensity will be given to form the modified Stern-Volmer equation to evaluate the complexing parameters, including conditional stability constants [34, 35]:

$$F_0/(F_0\text{-}F) = 1/(f_a K_a[\text{Sb(III)}]) + 1/f_a \quad (2)$$

...where F_0 and F are the fluorescence intensity in absence and presence of the quencher, (Sb(III)), respectively; K_a is

the Stern-Volmer quenching constant of the accessible fraction, i.e. conditional stability constant; f_a represents the fraction of the initial fluorescence, which is accessible to the quencher (Sb(III)); and [Sb(III)] is the concentration of Sb(III).

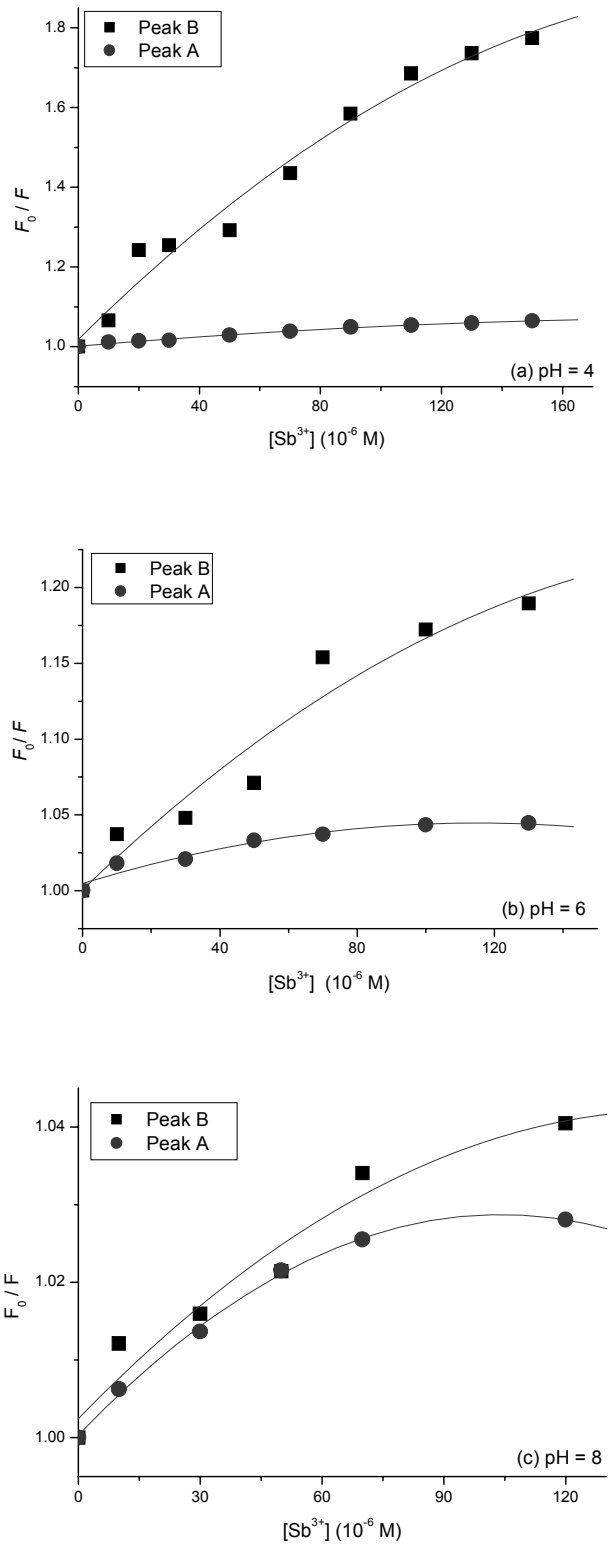

Fig. 3. Stern-Volmer plots of fluorescence quenching of EPS titrated with a Sb(III) solution at various pHs. (a) at pH 4; (b) at pH 6 and (c) at pH 8.

All the fluorescence titration data at pH 4.6 and 8 were well fitted with the modified Stern-Volmer equation (R^2 =0.941-0.992). The quenching parameters for EPS by Sb(III) at various pHs are listed in Table 1. The change of values of logK_a and f_a for peak B was larger than that for peak A with increasing pH. All values of f_a for peak B were higher than those for peak A at various pHs. The value of logK_a showed a contrary trend with pH change to that of f_a. This indicates that the proportion of the accessible fluorophore for peak A was higher than that of peak B. However, the fluorephore A-Sb(III) complexes were more stable than fluorephore B-Sb(III) complexes. The values of logK_a for the EPS-Sb(III) system (3.21-4.13) were close to those for the EPS-Hg(II) system (3.28-4.48) [30]. The values logK_a for the EPS-Sb(III) system were also close to those for other metals binding to EPS that were determined using other methods [36, 37]. For example, using the polargraphic method, Comte et al. [36] determined the conditional binding constants for Cu(II), Pb(II), and Cd(II) to EPS from activated sludges to be 3.2-4.5, 3.9-5.7, and 3.7-5.0, respectively.

Binding Constants and Binding Bites Numbers

The binding constant (K_b) and binding site number n were calculated from equation (3) [38]:

$$\log[(F_0\text{-}F)/F] = \log K_b + n\log[\mathrm{Sb(III)}] \qquad (3)$$

...where F_0 and F are the fluorescence intensities of fluorophores in the absence and presence of Sb(III), respectively. K_b is the binding constant, n the number of binding sites, and [Sb(III)] the Sb(III) concentration.

The values of logK_b, n, and the correlation coefficients were listed in Table 2. For peak A, the values of logK_b and n decreased with increasing solution pH. This means that fluorophores A (tyrosine) have greater binding capacity and more classes of binding sites for Sb(III) under acidic conditions. For peak B, the maximum values of logK_b and n were observed under neutral conditions and decreased a little when the solution turned out to be acidic or basic, indicating that protein-like substances in EPS were prone to complexation with Sb(III) under neutral conditions. On the whole, the values of logK_b peak A were greater than that for peak B. This suggests that fluorophores A in EPS have stronger affinity for Sb(III) than fluorophores B. The values of n for peaks A and B were less than 1, denoting the presence of several classes of binding sites of EPS for complexation with Sb(III).

Binding Mode of Sb(III) to EPS

Fluorescence quenching is generally driven by four types of force, including hydrogen bonds, van der Waals forces, and electrostatic and hydrophobic interactions. When the enthalpy change (ΔH) could be regarded as a constant with temperature varying within a narrow range [39], Van't Hoff equation [40] was employed to determine the thermodynamic parameters.

Table 1. The calculated complexation parameters at peaks A and B for EPS at various pH ($p<0.0001$).

pH	Peak A				Peak B			
	K_a (M^{-1})	logK_a	f_a	R^2	K_a (M^{-1})	logK_a	f_a	R^2
4	8320.29	3.92	0.451	0.974	8096.49	3.91	0.865	0.952
6	10182.76	4.01	0.088	0.954	1606.03	3.21	0.995	0.941
8	13611.37	4.13	0.048	0.968	2906.41	3.46	0.188	0.961

Table 2. The calculated binding constants, logK_b and binding site numbers, *n,* for peaks A and B at various pH ($p<0.0001$).

pH	Peak A			Peak B		
	logK_b	*n*	R^2	logK_b	*n*	R^2
4	4.14	0.809	0.918	3.37	0.583	0.801
6	3.77	0.706	0.961	3.72	0.469	0.968
8	3.31	0.665	0.905	3.22	0.613	0.968

Table 3. The thermodynamic parameters for the EPS-Sb(III) system ($p<0.0001$).

Peak	*T* (K)	EPS			
		ΔG	*ΔH*	*ΔS*	R^2
		(KJ·mol^{-1})	(KJ·mol^{-1})	(J K^{-1}·mol^{-1})	
Peak A	288	-19.3951	-33.42	-48.71	0.9999
	293	-19.1516			
	298	-18.9080			

Complexation of EPS with Sb(III) in nature was a thermodynamic process.

$$\ln K = -\Delta H/RT + \Delta S/R \quad (4)$$

...where R is the universal gas constant (8.314 J^{-1}·mol^{-1}), *T* is the absolute temperature (*K*), and *K* is the binding constant at the corresponding temperature. Δ*G* was calculated from equation (5):

$$\Delta G = \Delta H - T\Delta S \quad (5)$$

The values of the Gibbs free energy change (Δ*G*), the enthalpy change (Δ*H*), and the entropy change (Δ*S*) are presented in Table 3.

The negative values Δ*G* and Δ*S* indicate that the interaction of the fluorophores in EPS and Sb(III) is a spontaneous and endothermic process. Δ*H*<0 and Δ*S*<0 suggested that the binding of Sb(III) to fluorophores in EPS is driven

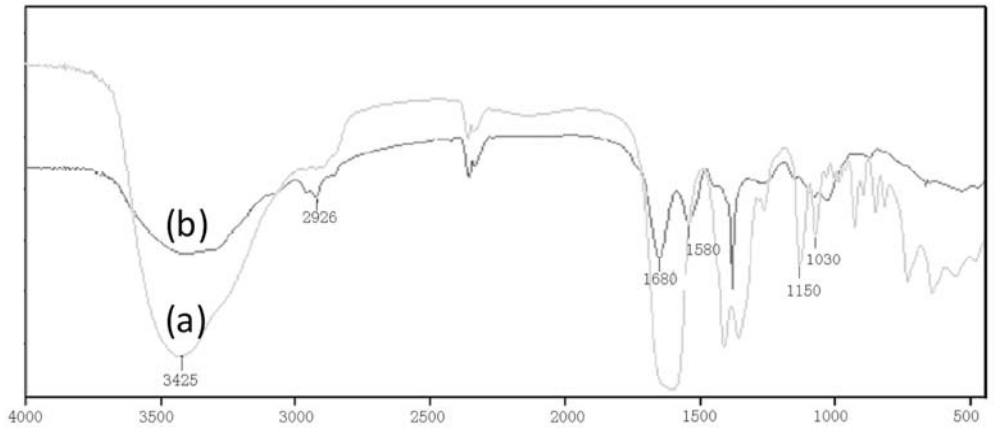

Fig. 4. FT-IR spectra of EPS before (a) and after (b) binding with Sb(III) at pH 6.

by the hydrogen bonding and Van der waals interactions in low dielectric medium [40, 41].

FTIR Spectroscopy Analysis

Fig. 4 shows FTIR spectra of EPS before and after binding with Sb(III). A broad peak at 3,425 cm^{-1} of stretching of O-H bond indicated the hydroxyl functional groups. The peaks at 1,680 and 1,580 cm^{-1} correspond to the amide I (C=O stretching) and amide II groups (N-H bending and C-N stretching), respectively. The spectra bands between 1,150 and 1,030 cm^{-1} exhibit polysaccharide groups [41, 42], indicating that carbohydrates were present in the EPS. The results coincided with FTIR spectra character of EPS extracted from biofilms and activated sludges [18, 41, 43-45]. The functional groups belonging to the fingerprint region might be assigned to the phosphate group, which is one of the functional groups of which nucleic acids are composed. In the FTIR spectra of EPS bound Sb(III), peak intensity and peak position of amide I and amide II changed. This also confirmed the complexation of the protein substances in EPS with Sb(III). It was observed that hydroxyl functional groups and carbohydrate groups were involved in the complexation of EPS with Sb(III). This information could not be attained in the EEM because polysaccharides do not show fluorescent properties. Although EEM fluorescence spectroscopy provides important information on interaction of EPS and metal ions in aqueous media, it cannot provide any information about the nonfluorescent substances.

Conclusions

This study shows that EEM spectroscopy is a novel tool for studying the chemical properties of EPS and its complexation with metal ions. The following conclusions can be made from this study:

(1) Two protein-like peaks were identified in the EEM spectra of EPS samples. Fluorescence of peaks A and B for EPS can be quenched by Sb(III).

(2) The modified Stern-Volmer equation can well depict the fluorescence quenching titration. The quenching constants ($\log K_a$) and the binding constants ($\log K_b$) were in the range of 3.21-4.13 and 3.22-4.14, respectively.

(3) Binding of Sb(III) to EPS was spontaneous and endothermic. The hydrogen bonding and Van der waals forces play a crucial role in binding of Sb(III) to EPS.

(4) FT-IR confirmed that polysaccharides in EPS also participated in complexation EPS with Sb(III) besides protein-like substances.

Acknowledgements

This work was supported by the Program of 100 Distinguished Young Scientists of the Chinese Academy of Sciences, and the National Natural Science Foundation of China (U1120302 , 21177127, and 41203088).

References

1. UNITED STATES ENVIRONMENTAL PROTECTION AGENCY. Water Related Fate of the 129 Priority Pollutants, vol. 1. USEPA, Washington, DC, USA, EP-440/4-79-029A. pp. 23-29, **1979**.
2. DE BOECK M., KIRSCH-VOLDERS M., LISON D. Cobalt and antimony: genotoxicity and carcinogenicity. Mutat. Res-Fund Mol. M. **533**, 135, **2003**.
3. HUANG H., SHU S.C., SHIH J.H., KUO C.J., CHIU I.D. Antimony trichloride induces DNA damage and apoptosis in mammalian cells. Toxicol., **129**, 113, **1998**.
4. ZHANG D.Y., PAN X.L., MU G.J., WANG J.L. Toxic effects of antimony on photosystem II of *Synechocystis* sp. as probed by in vivo chlorophyll fluorescence. J. Appl. Phycol. **22**, 479, **2010**.
5. PAN X.L., ZHANG D.Y., CHEN X., BAO A.M., LI L.H. Antimony Accumulation, Growth Performance, Antioxidant Defense System and Photosynthesis of *Zea mays* in Response to Antimony Pollution in Soil," Water Air Soil Pollut. **215**, 517, **2011**.
6. PAN X.L., ZHANG D.Y., CHEN X., LI L.H., MU G.J., LI L., SONG W.J. Sb uptake and photosynthesis of *Zea mays* growing in soil watered with Sb mine drainage: an OJIP chlorophyll fluorescence study. Pol. J. Environ. Stud. **19**, (5), 981, **2010**.
7. ZHU J., WU F.C., DENG Q.J., SHAO S.X., MO C.L., PAN X.L., LI W., ZHANG R.Y. Environmental characteristics of water near the Xikuangshan antimony mine, Hunan province. Acta scientiae Circumstantiae, **29**, 655, **2009**.
8. HE M.C., JI H.B., ZHAO C.Y., XIE J., WU X.M., LI Z.F. Preliminary studies of heavy metal pollution in soil and plant near antimony mine area. J. Beijing Normal Univ. (Natural Science). **38**, 417-420, **2002**.
9. VOLESKY B. Biosorption and me. Water Res. **41**, (18), 4017, **2007**.
10. LODEIRO P., REY-CASTRO C., BARRIADA J.L., DE VICENTE M.E.S. HERRERO R. Biosorption of cadmium by the protonated macroalga *Sargassum muticum*: Binding analysis with a nonideal, competitive, and thermodynamically consistent adsorption (NICCA) model. J. Colloid Interface Sci., **289**, 352, **2005**.
11. NAJA G., MUSTIN C., BERTHELIN J., VOLESKY B. Lead biosorption study with *Rhizopus arrhizus* using a metal-based titration technique. J. Colloid Interface Sci. **292**, 537, **2005**.
12. WANG J.L. Biosorption of copper(II) by chemically modified biomass of *Saccharomyces cerevisiae*. Process Biochem. **37**, 847, **2002**.
13. HO Y.S, MCKAY G. Sorption of dyes and copper ions onto biosorbents, Process Biochem. **38**, 1047, **2003**.
14. GUPTA V.K., RASTOGI A., NAYAK A. Adsorption studies on the removal of hexavalent chromium from aqueous solution using a low cost fertilizer industry waste material. Journal of Colloid and Interface Science. **342**, 135, **2010**.
15. PAL A., PAUL A.K. Microbial extracellular polymeric substances: central elements in heavy metal bioremediation. Indian J. Microbiol. **48**, 49, **2008**.
16. LIU Q.S., TAY J.H., LIU Y. Substrate concentration-independent aerobic granulation in sequential aerobic sludge blanket reactor. Environ. Technol. **24**, 1235, **2003**.
17. PAN X.L., LIU J., ZHANG D.Y., CHEN X., SONG W.J., WU F.C. Binding of dicamba to soluble and bound extracellular polymeric substances (EPS) from aerobic activated sludge: A fluorescence quenching study. J. Colloid Interface Sci. **345**, 442, **2010**.

18. ZHANG D.Y., WANG J.L., PAN X.L. Cadmium sorption by EPS produced by anaerobic sludge under sulphate-reducing conditions. J. Haz. Mat. **138**, 589, **2006**.
19. LIU Y., LAM M.C., FANG H.H. Adsorption of heavy metals by EPS of activated sludge. Water Sci. Technol. **43**, 59, **2001**.
20. TOURNEY J., NGWENYA B.T., MOSSELMANS J.W.F., MAGENNIS M. Physical and chemical effects of extracellular polymers (EPS) on Zn adsorption to Bacillus licheniformis S-86. J. Colloid Interface Sci., **337**, 381, **2009**.
21. SU X.F., WANG S.G., ZHANG X.M., CHEN P.J., LI X.M., GAO B.Y., MA Y. Spectroscopic study of Zn^{2+} and Co^{2+} binding to extracellular polymeric substances (EPS) from aerobic granules. J. Colloid Interface Sci. **335**, 11, **2009**.
22. ZHANG D.Y., PAN X.L., MU G.J. Biosorption of antimony (Sb) by the cyanobacterium *Synechocystis* sp. Pol. J. Environ. Stud. **20**, (5), 1353, **2011**.
23. STANIER R.Y., KUNISAWA R., MANDEL M., COHEN-BAZIRE G. Purification and properties of unicellular blue-green algae (order Chroococcales). Bacteriol. Rev. **35**, 171, **1971**.
24. LIU H., FANG H.P. Extractions of extracellular polymeric substances (EPSs) of sludges, J. Biotechnol. 95, 249, 2002.
25. COMTE S., GUIBAUD G., BAUDU M. Biosorption properties of extracellular polymeric substances (EPS) resulting from activated sludge according to their type: Soluble or bound. Process Biochem. **41**, 815, **2006**.
26. DUBOIS M., GILLES K.A., HAMILTON J.K., REBERS P.A., SMITH F. Calorimetric method for determination of sugars and related substances. Anal. Chem. **28**, 350, **1956**.
27. BRADFORD M. M. A rapid and sensitive method for the quantitation of microgram quantities of protein utilizing the principle of protein-dye binding. Anal. Biochem. **72**, 248, **1976**.
28. SHENG G.P., YU H.Q. Characterization of extracellular polymeric substances of aerobic and anaerobic sludge using three-dimensional excitation and emission matrix fluorescence spectroscopy. Water Res. **40**, 1233, **2006**.
29. CHEN W., WESTERHOFF P., LEENHEER J.A., BOOKSH K. Fluorescence excitation-emission matrix regional integration to quantify spectra for dissolved organic matter. Environ. Sci. Technol. **37**, 701, **2003**.
30. ZHANG D.Y., PAN X.L., MOSTAFA K.M.G., CHEN X., WU F.C., MU G. J., LIU J., SONG W. J., LIU Y.L., FU Q.L. Complexation between Hg(II) and biofilm extracellular polymeric substances: An application of fluorescence spectroscopy. J. Hazard. Mater. **175**, 359, **2010**.
31. ADAV S.S., LEE D.J. Extraction of extracellular polymeric substances from aerobic granule with compact interior structure. J. Hazard. Mater. **154**, 1120, **2008**.
32. PATEL-SORRENTINO N., MOUNIER S., BENAIM J.Y. Excitation- emission fluorescence matrix to study pH influence on organic matter fluorescence in the Amazon basin rivers. Water Res. 2371, **2002**.
33. LAKOWICZ J.R., Principles of Fluorescence Spectroscopy, third ed., Springer, Newyork, **2006**.
34. ESTEVES DA SILVA J.C.G., MACHADO A.A.S.C., OLIVEIRA C.J.S. Fluorescence quenching of anthropogenic fulvic acids by Cu(II), Fe(III) and UO_2^{2+}. Talanta **45**, 1155, **1998**.
35. LU X.Q., JAFFE R. Interaction between Hg(II) and natural dissolved-organic matter: a fluorescence spectroscopy based study. Water Res. **35**, 1793, **2001**.
36. COMTE S., GUIBAUD G., BAUDU M. Biosorption properties of extracellular polymeric substances (EPS) towards Cd, Cu and Pb for different pH values. J. Hazard. Mater. **151**, 185, **2008**.
37. GUIBAUD G., TIXIER N., BOUJU A., BAUDU M. Use of a polarographic method to determine copper, nickel and zinc constants of complexation by extracellular polymers extracted from activated sludge. Process Biochem. **39**, 833, **2004**.
38. HILL T.L. Cooperativity: Theory in Biochemistry, Springer-Verlag, New York, NY. **1985**.
39. ZHANG Y.Z., ZHOU B., LIU Y.X., ZHOU C.X., DING X.L., LIU Y. Fluorescence Study on the Interaction of Bovine Serum Albumin with P-Aminoazobenzene. J. Fluoresc. **18**, 109, **2008**.
40. ROSS P.D., SUBRAMANIAN S. Thermodynamics of protein association reaction: forces contribution to stability, Biochem. **20**, 3096, **1981**.
41. WANG Z.W., WU Z. C., TANG S. J. Extracellular polymeric substances (EPS) properties and their effects on membrane fouling in a submerged membrane bioreactor. Water Res. **43**, 2504, **2009**.
42. CROUE J.P., BENEDETTI M.F., VIOLLEAU D., LEENHEER J.A. Characterization and Copper Binding of Humic and Nonhumic Organic Matter Isolated from the South Platte River: Evidence for the Presence of Nitrogenous Binding Site. Environ. Sci. Technol. **37**, 328, **2003**.
43. GUIBAUD G., COMTE S., BORDAS F., DUPUY S, BAUDU M. Comparison of the complexation potential of extracellular polymeric substances (EPS) extracted from activated sludges and produced by pure bacteria strains, for cadmium, lead and nickel. Chemosphere **59**, 629, **2005**.
44. LARTIGES B.S., DENEUX-MUSTIN S., VILLEMIN G., MUSTIN G., BARRES O., CHAMEROIS M., GERARD B., BABUT M. Composition, structure and size distribution of suspended particulates from the Rhine river. Water Res. **35**, 808, **2001**.
45. MECOZZI M., ACQUISTUCCI R., DI NOTO V., PIETRANTONIO E., AMICI M., CARDIRILLI D. Characterization of mucilage aggregates in Adriatic and Tyrrhenian Sea: structure similarities between mucilage samples and the insoluble fractions of marine humic substance. Chemosphere **44**, 709, **2001**.